

Assessment of the expected seismic damage in the aggregated masonry buildings of the late XIX century of Barcelona, Spain

R. Moreno-González & J.M. Bairán

Universitat Politècnica de Catalunya (UPC), Spain



SUMMARY:

This paper aims at the evaluation of expected seismic damage of aggregated masonry buildings system, formed by a line of buildings along of the street; real buildings were studied of whom structural drawings were available. Each structure was individually built without any gaps between them, producing interaction among the buildings under lateral loads. Numerical model consists of 7 buildings: 5 in-row with rectangular shape and 2 corners (in the intersection of two streets) with a pentagonal shape.

Damage probability matrices were obtained from pushover analysis using the capacity and fragility curves. Seismic hazard is considered for the acceleration of Barcelona. Four damage states were considered: slight, moderate, extensive and complete (collapse).

The results showed that aggregated system analysed presents slight damage in a hard soil while very extensive damage occur in soft soil, furthermore, the expected seismic damage is high considering the low seismic action of Barcelona.

Keywords: seismic damage, aggregated buildings, vulnerability, unreinforced masonry, capacity spectrum method.

1. INTRODUCTION

Most of the losses due to earthquakes have their origin in the bad seismic behaviour of structures, high concentration of population, buildings, infrastructures, and exposed values increase the seismic risk in urban areas. Furthermore, advances in structural design are applied to new structures and, to a smaller extent, to the rehabilitation of existing ones. Therefore, the incorporation of a methodology to analyse the vulnerability and the expected seismic damage of existing buildings is important and necessary.

In this work, a method based on the capacity spectrum (ATC-40, 1996; Freeman, 1998; HAZUS-99, 1999; Fajfar, 2000; Milutinovic and Trendafiloski, 2003) is used to characterize the vulnerability and the expected damage of the unreinforced masonry buildings (URMB) of the city of Barcelona, Spain.

Barcelona is the second largest city of Spain, it is divided into 10 districts being the district *l'Eixample* the second oldest of the city, which is one of the most emblematic districts and with an important historic and architectonic value; it was designed at the end XIX century and the beginning of XX (took place between 1860 and 1940) and it is a reference of the modern urbanism. The *Eixample* district has the maximum average density, it covers 12,370 square meters with 520 blocks and with an average of 25 buildings for each block. Many buildings are not isolated, but they are part of aggregates of buildings forming blocks (Moreno, 2006).

The main objective of this paper is to evaluate the seismic damage of unreinforced masonry aggregated system (MAS) buildings built during the modernism (1890-1910) and post-modernism (1910-1936) period which are a distinguished characteristic of urbanistic heritage of the city. The seismic damage analysis of 1 side of squared blocks is considered with the goal of obtaining the

damage probability matrices for MAS buildings. The buildings models are built based on detailed data obtained from drawings and projects of existing structures; these buildings have an average age of 80 years and, hence, they have been designed and built without the consideration of any seismic resistant criterion.

The seismic action used to assess the seismic damage of this typology has been considered according to the basic seismic acceleration defined in the Spanish code (NCSE-02, 2002) for the city of Barcelona and the elastic response spectra defined in Eurocode EN-1998 (CEN, 2004).

Seismic capacity is evaluated from pushover analysis by means of bilinear capacity curve and fragility curves. Four damage states were considered: slight, moderate, extensive (severe damage) and complete (collapse). The damage probability matrices were obtained from the performance point and the fragility curves.

2. THE BUILDINGS

The construction system of the *Eixample* district is based in repetitive buildings models with certain differences, forming an autochthone construction system. The blocks are almost symmetrically square sizing about 113.3m×113.3m, they are perfectly aligned and they are bevelled in their vertices by edges of about 20m (with 45° angled corner of each block). The walls of the street façade, of the interior courtyard of the block and the walls between buildings are the main bearing walls. Each building may contain cores around the staircases and small internal courtyards made to provide natural light to the internal rooms.

In general, the URMBS are rectangular in plan, usually there exist one or more cores in the central part of the building, partially enclosed by brick walls of 10cm thick, formed around stair walls or courtyards. The façades walls work as load bearing elements together with a set of load interior walls, parallel to them. In the corner buildings, the plan geometry is trapezoidal in order to fit in the geometry of the block (Mari et al., 2003). Average building heights ranges between 6 to 8 storeys and 22m to 24m. A more detailed description of this typology can be found in Moreno (2006).

A building by building analysis was conducted, in which three models of real existents buildings were analysed in their 2 main directions (parallel and perpendicular to the street). The aggregated system was composed of 7 real structures: CB1+LB1+LB2+LB3+LB4+LB5+CB2 (5 centrals, LB, and 2 corners, CB). Fig. 2.1 shows an example of masonry aggregated system (MAS) buildings that define one of the four lines of a typical block and the line of buildings here studied.

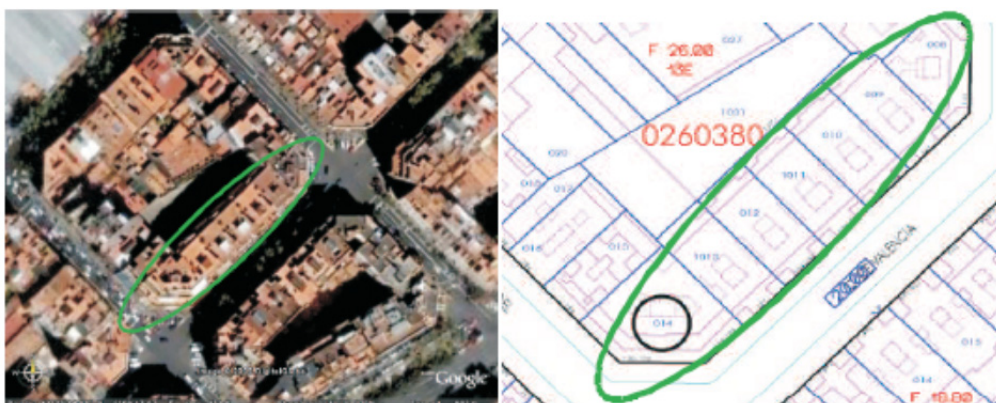


Figure 2.1. Aggregated system buildings analyzed in the *Eixample* district

The CB building was built in 1940, it has 3 sections of façade, 2 they are in each street of the crossing and 1 it is in the bevel, the walls are located in parallel to create the resisting system. The main and

back façades have thickness of 0.40m and 0.30m, respectively, the interior walls have 0.15m of thickness, furthermore, the interior resisting system consists on metallic beams and columns in the base and first floors. The area is 557m² and the perimeter of 94.30m (Moreno and Bairán, 2011). They are CB1 and CB2.

The LB buildings have a rectangular plan configuration and there are 2 types, the narrow (width<15m) and wide (width≥ 15m) buildings; these two structures have the main façade in the same line of the street. The narrow building has in plane dimensions of 12.65x27.0m (A=341.55m²), the main façade has maximum thickness of 0.50m and back façade has 0.45m of thickness, reducing from the first storey 10cm and 15cm, respectively. Laterals walls have 0.30m of thickness in the base floor and 0.15m in higher floors and the interior walls have 0.15m of thickness. The year of construction was 1930-1931. They are LB2, LB3 and LB4. In the wide building the walls have 0.15m of thickness and the façades 0.30m. In the base and first floor there are metallic beams and columns, which support the weight of the superior walls (Moreno and Bairán, 2011). It was built between 1882-1886 and the in plane dimension is 18.4mx23.7m (A=436.08m²). They are LB1 and LB5.

Table 2.1 shows the different height of the three type models of buildings chosen to model the MAS buildings. The floor system is unidirectional and can be made of wooden, steel or precast concrete beams with small ceramics or mortar vaults in between, depending on the building period, showing a poor stiffness both to bending moment and to axial forces. The floors were considered as timber with the structural configuration described in Fig 2.2.

Table 2.1. Summary description of the buildings.

	CB1, CB2	LB2, LB3, LB4	LB1, LB5
H total (m) / storeys	22.4 (8 storeys)	22.0 (7 storeys)	24.4 (6 storeys)
H base floor (m)	3.1	4.0	4.8
H first floor (m)	2.5	3.0	4.0
H higher floors (m)	2.8	3.0	3.9

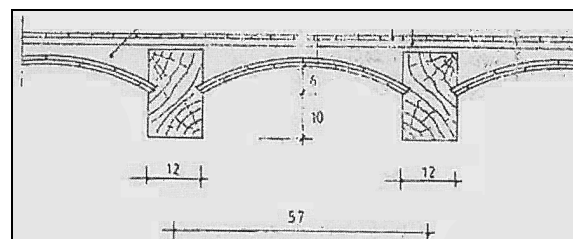


Figure 2.2. Timber floor

In base to the technical specifications of use, expert opinions and previous studies realized by some researchers in this typology (Yépez, 1996, Moreno et al., 2003), the mechanical parameters were defined as follows. The properties of the masonry walls were: Elastic modulus, $E=1800\text{N/mm}^2$, Shear modulus, $G=700\text{N/mm}^2$, compression strength, $f_{mk}=4.0\text{N/mm}^2$, Shear strength, $\tau_k=0.12\text{N/mm}^2$, Specific weight, $\gamma=18.0\text{kN/m}^3$. The properties of the timber floor are: Elastic modulus, $E_1=4000\text{N/mm}^2$, Elastic modulus, $E_2=40\text{N/mm}^2$, Shear modulus, $G=300\text{N/mm}^2$. Finally, the metallic profiles elements are HEB-200 for the columns and IPN-360 for the beams, and their mechanical properties are Elastic modulus, $E_s=2.1\text{E}5\text{N/mm}^2$, Specific weight, $\gamma=78.50\text{kN/m}^3$, Area, $A_{HEB-200}=0.00781\text{m}^2$, Inertia moment, $I_{Y_{HEB-200}}=56.97\text{E}-6\text{m}^4$, $A_{IPN-360}=0.00097\text{m}^2$ and $I_{Y_{IPN-360}}=19.61\text{E}-5\text{m}^4$.

2.1. TreMuri program

The different structural models were analysed using TreMuri program, developed in *Università degli Studi di Genova* (Genoa, Italy) by Galasco et al. (2002). This program allows 3D non-linear static and dynamic analysis of masonry structures combined with elements of other materials such as, for

instance, wood, iron or reinforced concrete, that are part of walls, beams or columns. It is a useful tool for study the nonlinear in-plane mechanical behaviour of masonry panels and to assess the expected damage for masonry buildings due to earthquakes.

Masonry panels are represented by means of a non linear macroelement model proposed by Gambarotta and Lagomarsino (1993; 1997) which allows for the needed accuracy of masonry buildings without heavy computational cost. This formulation considers shear-sliding damage evolution, which controls the strength deterioration (softening) and the stiffness degradation (Penna, 2002; Galasco et al., 2004). A more detailed description of the TreMURI program can be found in Lagomarsino et al. (2008).

3. CAPACITY ASSESSMENT

A building can be characterised by its capacity curve obtained by means of a pushover analysis, which allows obtaining the base shear versus top displacement curve. Capacity curve is transformed into the capacity spectrum in which vertical axis represent the spectral acceleration (Sa) and the horizontal axis represent the spectral displacement (Sd); this spectrum can be represented in bilinear form in order to define objective structural parameters such as ductility, yielding and ultimate points, etc., see figure in Table 3.1. These parameters are further used to build the fragility curves, which relate the probability of certain damage states for a seismic action. In this study, the seismic action is characterized by the spectral displacement, which is considered to be plausibly related to the expected damage.

In this work, the fragility curves are defined according to Eqn. 3.1 under the assumption that they following a log-normal probability distribution (HAZUS-99, 1999; Milutinovic and Trendafiloski, 2003) and they are defined as the graphical representation of the cumulative probability density function of reaching or exceeding a certain damage limit state for the spectral displacement, which represents the intensity of the seismic action.

$$P[DS/Sd] = \Phi \left[\frac{1}{\beta_{DS}} \cdot \ln \left(\frac{Sd}{\overline{Sd}_{DS}} \right) \right] \quad (3.1)$$

\overline{Sd}_{DS} is the mean spectral displacement for which the probability of having a determined damage state is 50%. β_{DS} is the coefficient of variation of the natural logarithm of the spectral displacement for the damage limit state under consideration damage state (DS). Φ is the normal cumulative distribution function and Sd is the spectral displacement. Subscript DS indicates the considered damage; these damage states have the same meaning as in Barbat et al. (2008).

Table 3.1. Damage state thresholds.

DS	Damage state	Thresholds \overline{Sd}_{DS}	β_{DS}
1	Slight	$0.7 \cdot D_y$	0.99
2	Moderate	D_y	0.97
3	Extensive	$D_y + 0.25 \cdot (D_u - D_y)$	0.90
4	Complete	D_u	0.88

Each fragility curve requires the definition of the damage threshold (\overline{Sd}_{DS}) of the specific damage state and the variability associated with it, β_{DS} . The determination of the damage thresholds are defined in Table 3.1 in terms of yielding (D_y) and ultimate (D_u) displacements using the bilinear capacity

spectrum and the conditions defined there. In HAZUS methodology (HAZUS-99, 1999) the coefficients of deviation (β_{DS}) are defined for different typologies and they are based on numerical trials and expert opinion. For the typology studied the values of β_{DS} used are given in Table 3.1 (Moreno and Bairán, 2011).

3.1. Modal analysis

The buildings were analysed in two orthogonal directions considered as isolated from the others. After modal analysis, the modal participation factor (Γ) and the vibration natural period (T) corresponds to the displacements main were calculated. Table 3.2 shows the vibration mode, where U_X is the displacement parallel to the street and U_Y is the displacement perpendicular to the street, and the modal participation factor (MPF) for both directions. In the Y direction, mode 1 was used for the analysis of CB, while mode 3 was considered for LB.

Table 3.2. Vibration natural period and MPF for CB and LB.

Models	T (s)		Γ_Y	Γ_X
CB1 – CB2	0.808 - Mode 1 (U_Y)	0.827 - Mode 2 (U_X)	1.544	1.551
LB2 – LB3 – LB4	0.846 - Mode 1 (U_X)	0.561 - Mode 3 (U_Y)	1.342	1.541
LB1 – LB5	1.246 - Mode 1 (U_X)	0.796 - Mode 3 (U_Y)	1.329	1.259

In the X direction – parallel to the street – no gap exists between the buildings; hence interaction between them is expected. The analysis in this direction was performed considering a masonry-aggregated-system (MAS) of one of the sides of the block, see Fig. 2.1. A plausible approximation of the MAS response can be obtained by superposition of response of each building for the above mentioned combination (CB1+LB1+LB2+LB3+LB4+LB5+CB2) where the period of vibration and mass participation factor for the equivalent SDOF were obtained as $T^*=0.861$ s and $\Gamma^*=1.451$.

3.2. Capacity curves

From pushover analysis the capacity curves are obtained. Fig. 3.1 shows the capacity curves in Y direction for the CB and LB and Fig. 3.2 shows it for the MAS model (X direction). Each graphic is represented in the ordinates, by the base shear/modal participation factor, and in abscises, by the displacement in the top/modal participation factor (MPF).

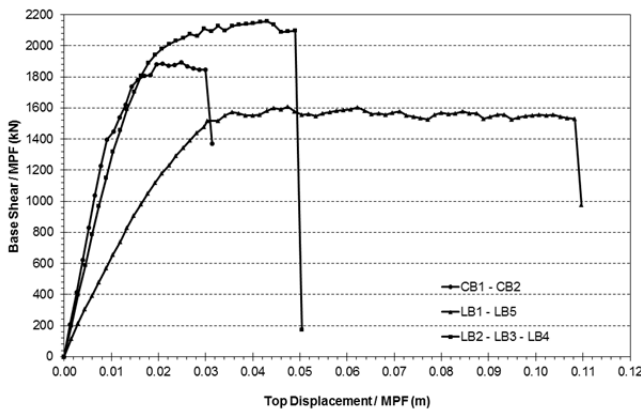


Figure 3.1. Capacity curves of isolated buildings

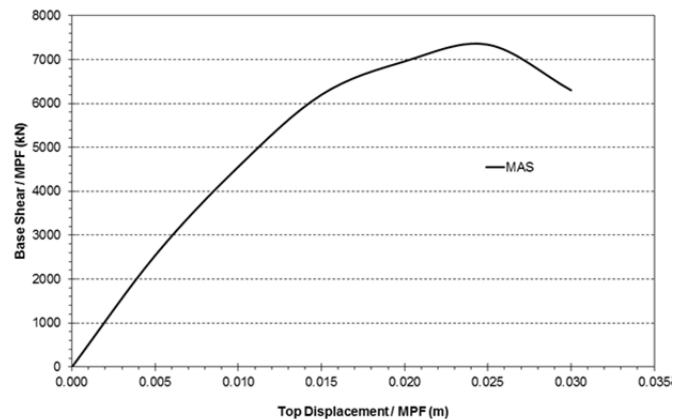


Figure 3.2. Capacity curves of aggregated buildings

Table 3.3 shows, in spectral coordinates, the yield and ultimate capacity points defining the bilinear capacity spectra of CB and LB analysed in both directions. A_y and A_u are the ordinates of D_y and D_u , respectively. Furthermore, Table 3.3 shows the points defining the bilinear capacity spectrum used to define the damage state threshold for the fragility curves for the aggregated system (MAS).

Table 3.3. Parameters of the bilinear capacity spectrum for URB.

Building Models	Yield capacity				Ultimate capacity			
	Direction Y		Direction X		Direction Y		Direction X	
	D_y (m)	A_y (g)	D_x (m)	A_x (g)	D_u (m)	A_u (g)	D_v (m)	A_v (g)
CB1 – CB2	0.012	0.119	0.014	0.1350	0.030	0.119	0.029	0.1370
LB2 – LB3 –LB4	0.017	0.193	0.019	0.0781	0.046	0.195	0.074	0.0928
LB1 – LB5	0.025	0.106	0.040	0.0655	0.108	0.106	0.068	0.0667
MAS	-	-	0.015	0.0800	-	-	0.030	0.0731

3.3. Fragility curves

Fragility curves are built from bilinear capacity spectrum. Table 3.4 shows the corresponding parameters to define the fragility curves for each model. Figs. 3.3, 3.4 and 3.5 show the fragility curves obtained for CB and LB and Fig. 3.6 shows the corresponding to MAS buildings.

Table 3.4. Parameters of the fragility curves for URB.

Building Models	Damage states thresholds			
	Slight \overline{Sd}_1 (m)	Moderate \overline{Sd}_2 (m)	Extensive \overline{Sd}_3 (m)	Complete \overline{Sd}_4 (m)
CB1 – CB2	0.0084	0.0121	0.0165	0.0300
LB2 – LB3 –LB4	0.0117	0.0167	0.0240	0.0460
LB1 – LB5	0.0175	0.0250	0.0458	0.1082
MAS	0.0105	0.0150	0.0188	0.0300

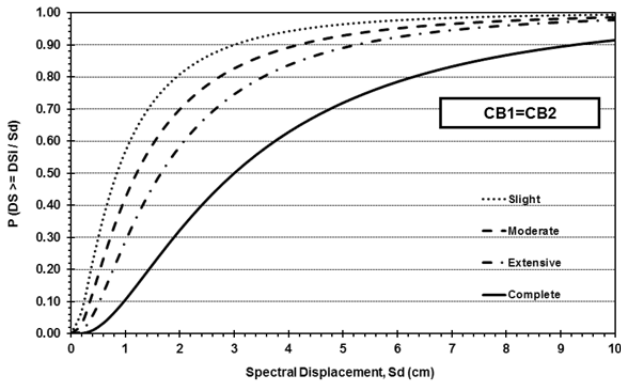


Figure 3.3. Fragility curves for CB1 - CB2 models

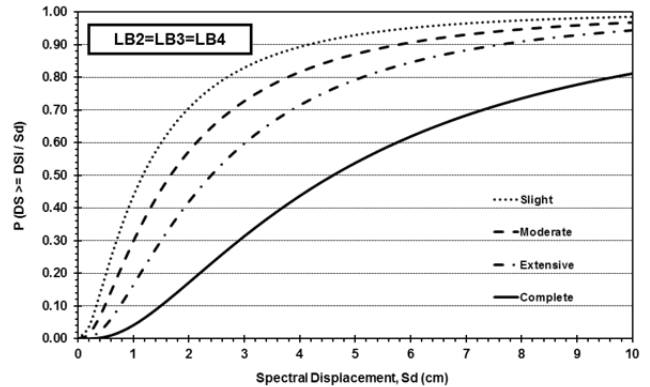


Figure 3.4. Fragility curves for LB2 - LB3 - LB4 models

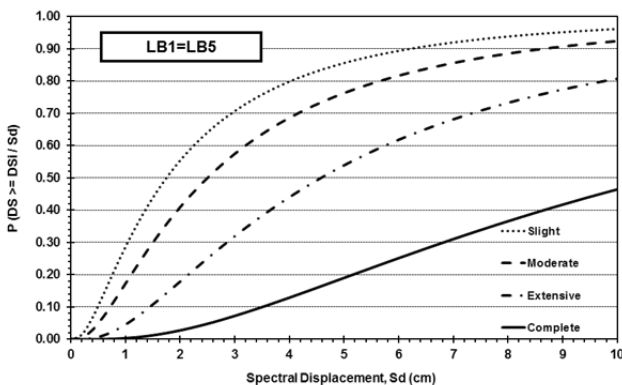


Figure 3.5. Fragility curves for LB1 - LB5 models

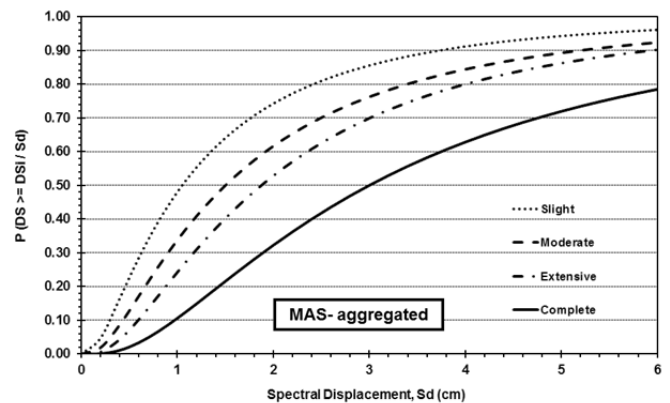


Figure 3.6. Fragility curves for MAS buildings

4. SEISMIC ASSESSMENT

The seismic behaviour of a building can be quantified by means of the performance point (Sd_{pp}), which is obtained from of capacity and demand spectra. The demand spectrum is obtained from the elastic response spectrum with 5% of the critical damping after a suitable reduction for larger effective damping take into account the inelastic behaviour, it is represented in Sd - Sa coordinates. There are different methods to obtain the demand spectrum and the performance point, the method described in annex B of the Eurocode 8 (CEN, 2004) is followed here to obtain them.

4.1. Seismic action

Barcelona is situated on the northeast Mediterranean coast and it is delimited by *Collserola* mountain, *Besòs* and *Llobregat* rivers and by the Mediterranean sea. The seismic action is defined in terms of 5% damped elastic response spectrum, in the Spanish seismic normative (NCSE-02, 2002) the basic seismic acceleration for Barcelona is 0.04g. The shape of the response spectra were related to each soil class as in Eurocode 8 (CEN, 2004), four types of soils: A, B, C and D were considered. Soil A corresponds to hard soils and D is soft soils, while C and B are made of intermediate soils. Fig. 4.1 shows the corresponding elastic response spectra used for the analysis and the parameters considered are given in Table 4.1, see Eurocode 8 (CEN, 2004).

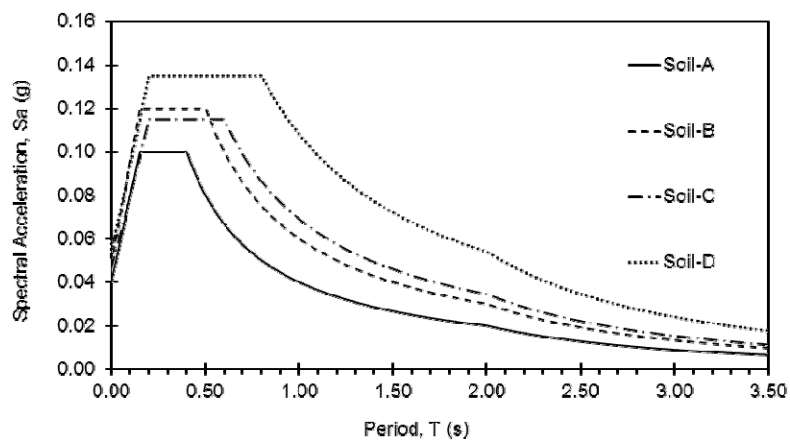


Figure 4.1. Elastic response spectra (Sa - T) used for Barcelona

Table 4.1. Parameters of the response spectra defined with the Eurocode 8.

Parameters	Definition	Soil A	Soil B	Soil C	Soil D
S	soil parameter	1.00	1.20	1.15	1.35
k_1	parameters that define the shape of the spectrum for periods of vibration major that T_c	1.00	1.00	1.00	1.00
k_2	parameters that define the shape of the spectrum for periods of vibration major that T_d	2.00	2.00	2.00	2.00
T_b (s)	define the limits of the plateau of constant acceleration	0.15	0.15	0.20	0.20
T_c (s)	define the limits of the plateau of constant acceleration	0.40	0.50	0.60	0.80
T_d (s)	define the initiation of the branch of constant displacement on the spectrum	2.00	2.00	2.00	2.00

4.2. Seismic demand

Table 4.2 shows, for the seismic demand considered, the corresponding Sd_{pp} for buildings CB, LB and for the MAS located in the different type of soils of Barcelona.

Table 4.2. Performance points, S_{dpp} (cm), for URMB.

Models	Soil A	Soil B	Soil C	Soil D
CB1 – CB2	0.63	0.94	1.09	2.15
LB2 – LB3 –LB4	0.58	0.87	1.03	2.15
LB1 – LB5	0.96	1.44	1.66	2.59
MAS	0.86	1.28	1.48	2.31

4.3. Damage probability matrices

The damage probability matrices (DPM) characterise the damage of a structure corresponding to the response seismic to the subjected. These DPM are obtained in order to get the probability of having a damage bellow or equal to the threshold. This is done by entering into fragility curve i with the performance point of the structure in order to obtain the probability of having a damage lower or equal to such damage state. The probability of having damage state i in the structure if thus obtained as the difference between the cumulative probability for damage threshold i and $i+1$. Table 4.3 shows the damage probability matrices for isolated structures, orthogonal to the street direction, and the aggregated system (MAS), parallel to the street, in the different zones. Fig. 4.2 shows a graphic representation of the damage probability for MAS buildings.

Table 4.3. Damage probability matrices in (%).

Soils	Models	0-No damage	1-Slight	2-Moderate	3-Extensive	4-Complete
Soil A	CB1-CB2	62	12	12	10	4
	LB2-LB3-LB4	76	10	8	5	1
	LB1-LB5	73	11	12	4	0
	MAS	58	14	9	11	8
Soil B	CB1-CB2	46	14	14	17	9
	LB2-LB3-LB4	61	13	12	11	3
	LB1-LB5	58	14	18	9	1
	MAS	42	14	11	17	16
Soil C	CB1-CB2	30	12	14	24	20
	LB2-LB3-LB4	42	14	16	19	9
	LB1-LB5	50	14	22	12	2
	MAS	35	14	9	19	23
Soil D	CB1-CB2	17	10	12	26	35
	LB2-LB3-LB4	27	13	15	25	20
	LB1-LB5	35	14	25	21	5
	MAS	21	11	9	31	28

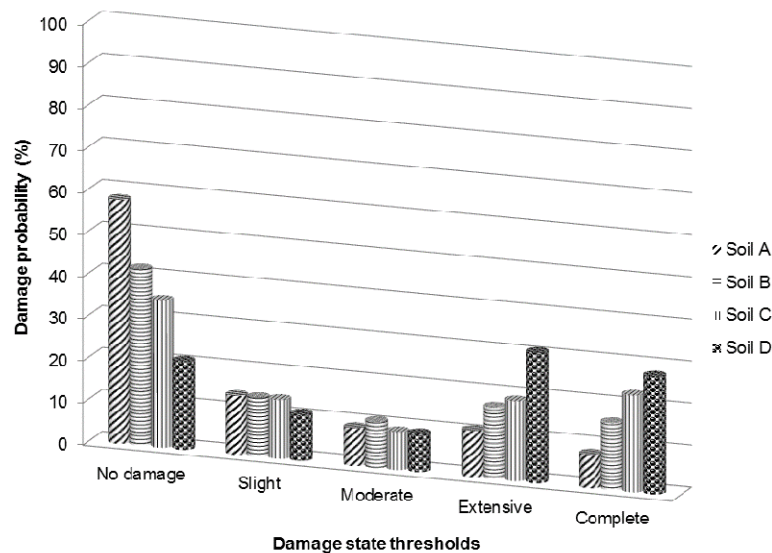


Figure 4.2. Probability of occurrence of the damage states for MAS

5. DISCUSSION AND CONCLUSION

As individual building, for the seismic scenario considered, the greatest damage probability expected (35%) corresponds to CB model located on soil type D and the minor expected damage probability (73-76% non damage and 0-1% complete) is obtained for the models LB placed in soil type A. This behaviour is maintained for all soil types. The reason for these extreme values could be due to the regularity in the distribution of walls of the line buildings and the irregularity of the corner building. In general, the damage increases with decreasing soil quality, the increase of the damage is spectacular in MAS buildings, which goes 58% of non damage in hard ground (soil A) and 21% in a soft soils (type D), see Fig. 4.2 and Table 4.3. Furthermore, it seems that MAS buildings inherit the lack of seismic resistance of the two corner buildings. It is concluded that, although the expected seismic demand is low ($PGA=0.04g$), the typical configuration of unreinforced masonry buildings present a high vulnerability and a significant expected seismic damage.

ACKNOWLEDGEMENTS

This work has been partially sponsored by the Spanish Ministry of Science and Innovation through the research project "Rehabilitation of Roads and Freeways: REHABCAR" (IPT-370000-2010-29). The first author gratefully acknowledges to the Prof. Sergio Lagomarsino and with all his work-team (*Università degli Studi di Genova*). The authors want to thank the support of Mr. Vicente Alegre (*COTCA, S.A.*) and the Department of Construction Engineering of the *UPC*.

REFERENCES

- ATC-40. Applied Technology Council. (1996). Seismic evaluation and retrofit of concrete buildings. Federal Emergency Management Agency (FEMA). Report: SSC 96-01. Vol. 1. Seismic Safety Commission. Redwood City, California.
- Freeman, S.A. (1998). Development and use of the capacity spectrum method. In: *Proceedings of the 11th European Conference on Earthquake Engineering*. Paris.
- HAZUS 99.(1999). HAZUS Technical manual. Federal Emergency Management Agency (FEMA) & National Institute of Building Sciences (NIBS). Volume 1,2,3. Washington, DC.
- Fajfar, P. (2000). A non linear analysis method for performance bases seismic design. *Earthquake Spectra*, 16:3,573-592.
- Milutinovic, Z.V. and Trendafiloski, G.S. (2003). Vulnerability of current buildings. Work Package 4 of the European RISK-UE Project Handbook: an advanced approach to earthquake risk scenarios with

- applications to different European towns. European Commission (contract: EVK4-CT-2000-00014).
- Moreno, R. (2006). Evaluación del riesgo sísmico en edificios mediante análisis estático no lineal. Aplicación a diversos escenarios sísmicos de Barcelona. Doctoral Thesis (in Spanish). Barcelona (Spain): Universitat Politècnica de Catalunya, Spain. <http://hdl.handle.net/10803/6247>.
- NCSE-02 Normativa. (2002). Norma de Construcción Sismorresistente: Parte General y Edificación, Real Decreto 997/2002, Boletín Oficial del Estado: 244, Madrid.
- Eurocode 8. (2004). Design of structures for earthquake resistance – Part 1: General rules, seismic actions and rules for buildings. Comité Européen de Normalisation. EN 1998-1:2004, CEN Brussels, December, 229 pp.
- Mari, A., Alegre, V., Gens, A. and Roca, P. (2003). Estudio preliminar sobre los posibles efectos de la construcción de un túnel para el tren de alta velocidad bajo los edificios situados entre las calles Mallorca, Valencia, Lepanto y Cartagena. *Technical Report*. Departamento de Ingeniería de la Construcción. Universidad Politécnica de Cataluña. Barcelona, Spain.
- Moreno-González, R. and Bairan, J.M. (2011). Seismic performance analysis of the masonry buildings, typical of the Eixample district of Barcelona. *Informes de la Construcción*, 63(524), 21-32. doi:10.3989/ic.10045.
- Yépez, F. (1996). Metodología para la evaluación de la vulnerabilidad y riesgo sísmico de estructuras aplicando técnicas de simulación. Doctoral Thesis (in Spanish). Universitat Politècnica de Catalunya, España.
- Moreno, R., Bonet, R., Barbat, A., Pujades, L., Penna, A. and Lagomarsino, S. (2003). Evaluación de la vulnerabilidad sísmica de estructuras de mampostería no reforzada. Aplicación a un edificio de la zona del Eixample en Barcelona (España). *Revista Internacional de Ingeniería de Estructuras*, 82, 91-120.
- Galaso, A., Lagomarsino, S. and Penna, A. (2002). TREMURI Program: Seismic Analysis of 3D Masonry Buildings. Università degli Studi di Genova. Genoa, Italy.
- Gambarotta, L. and Lagomarsino, S. (1993). A microcrack damage model for brittle materials. *International Journal of Solids and Structures*, 30, 177–98.
- Gambarotta, L. and Lagomarsino, S. (1997). Damage model for the seismic response of brick masonry shear walls. Part II: the continuum model and its applications. *Earthq Eng Struct Dyn*, 26, 441–462.
- Penna, A. (2002). A macro-element procedure for the non-linear dynamic analysis of masonry buildings. Doctoral Thesis. Politécnico di Milano, Italy.
- Galasco, A., Lagomarsino, S., Penna, A. and Resemini, S. (2004). Non-linear seismic analysis of masonry buildings. *13th World Conference on Earthquake Engineering*, paper 843, Vancouver, Canada.
- Lagomarsino, S., Galasco, A., Penna, A. and Cattari, S. (2008). TREMURI: Seismic analysis program for 3D Masonry buildings (User guide). Technical report. Università degli Studi di Genova, Genoa, Italy.
- Barbat, A.H., Pujades, L.G., Lantada, N. and Moreno, R. (2008). Seismic damage evaluation in urban areas using the capacity spectrum method: application to Barcelona. *Soil Dyn Earthq Eng*, 28, 10–11, 851–865. doi: 10.1016/j.soildyn.2009.12.014.